Hindawi
Shock and Vibration
Volume 2020, Article ID 8740941, 12 pages
https://doi.org/10.1155/2020/8740941

Research Article

High Frequency Modal Testing of the Multiblade Packets Using a Noncontact Measurement and Excitation System

C. H. Liu,[1] C. Zang,[1] F. Li,[1] and E. P. Petrov[2]

[1]*Nanjing University of Aeronautics and Astronautics, Nanjing, China*
[2]*University of Sussex, Brighton, UK*

Correspondence should be addressed to C. Zang; c.zang@nuaa.edu.cn

Received 15 November 2019; Accepted 3 February 2020; Published 27 February 2020

Academic Editor: Shuaishuai Sun

High cycle failure of blades and vanes caused by the vibration is one of the major causes reducing the lifetime of turbomachines. For multiblade packets, the failure may occur at vibrations with high frequencies that can reach up to tens of kHz. The experimental modal testing of blades is crucial for the validation of numerical models and for the optimization of turbomachine design. In this paper, the test rig and procedure for measurements of dynamic characteristics of lightweight multiblade packets in wide and high frequency ranges are developed. The measurements are based on a noncontact excitation and noncontact measurement method, which allows the determination of the modal characteristics of the packets with high accuracy in wide frequency ranges. The responses of the multiblade packets are measured using a Scanning Laser Doppler Vibrometry (SLDV), while vibrations are excited by the acoustic excitation technique. Modal tests of the blade packet comprising 18 vane blades connected by shrouds are performed. The measurements are performed within the high frequency range of 0–30 kHz, and the natural frequencies and mode shapes are obtained for first 97 modes. To capture the complex high frequency blade mode shapes, each blade in the packet is scanned over 25 reference points uniformly distributed over the blade concave surface. In order to obtain the high frequency resolution, the frequency range used for the measurements is split into several frequency intervals accordingly to the number of spectral lines available in the used data acquisition system, and for each such interval, the test is performed separately. The finite model of the packet is created, and the numerical modal analysis is performed to compare the calculated natural frequencies and mode shapes with the experimental measurements. The comparison shows the satisfactory with those from finite element analysis. It illustrates the measurement method described in this work is effective and reliable.

1. Introduction

The multiblade systems are widely applied in rotating machinery [1]. The accurate determination of vibration characteristics of blade assemblies is a significant part in design of turbomachines. The vibrations of rotating blades could cause the excessive stress levels and blade damage due to the localized vibrations of several blades and due to the coupling of vibration in multiblade systems [2, 3]. Therefore, the accurate knowledge of the characteristics of bladed assemblies is recognized to be crucial for the reliable operation of turbomachines and gas-turbine engines. In the past, many investigators applied uncoupled models to estimate natural frequencies and mode shapes of a single blade system, but multiblade assemblies have much more complex modal properties. The studies of blade packets are rather restricted in the literature, and one such study is published by Ewins and Imregun in [4] where they show that the vibration modes of a packet of cantilevered blades are rather different from a continuously shrouded bladed assemblies.

The free-vibration characteristics of a single cantilevered packet without disk effects were investigated using the finite-element method in [5]. Huang in [6] calculated the vibration characteristics of the coupled turbomachinery blades with various types of connecting elements by using the transfer matrix method. To reduce the size of equations in the model, Lim et al. [7] employed hybrid deformation variables and the Rayleigh-Ritz method to solve a simplified model of the multipacket blade system. Uchino et al. [8] and Delhelay [9] applied the finite element method to study the stress state in

a turbine disc assembly subjected to thermomechanical loading, and the results were verified using photoelastic stress analysis. Ma et al. [10] used a multiple parameters optimization with the response surface method for updating the finite element (FE) model of a blade swing mechanism in order to improve the correlation between the modes calculated from the FE model and those from the modal test. The effect of a damage caused by mistuning on the blade group natural frequencies was investigated in [11].

Although bladed disk assemblies have been studied for many years, the studies on multiblade packet vibrations are generally limited to the use of finite element methods or other mathematical methods, e.g., see [12, 13] and a review in [14]. Relatively little attention has been devoted to experimental investigation of blade packets. It is mainly due to the complexity of the modal characteristics of these structures and the difficulty in the measurement of mode shapes for such structure using conventional measurements techniques available a short time ago. The industrial practice shows that cracks and blade failure of multiblade packets are usually caused by the local vibrations of blades at high vibration frequencies. So, the experimental investigations of high-order modes for multiblade packets are of great significance.

Due to the complexity of the multiblade packets and their localized vibration mode shapes, it is essential to obtain the experimental vibration characteristics of multiblade packets by effective tests. However, it is not easy to conduct an accurate experiment for the lightweight multiblade packets when the traditional contact accelerometer is used for the vibration amplitude measurements, since the attachment of the accelerometer changes the dynamic characteristics of the blade packet. In addition, it is an enormous challenge to acquire the experimental modal shapes of the complex blade packets due to the necessity vibrations at very large number of measurement points needed to capture the possible mode localization over the whole packet and over each blade in the packet. Bertini et al. [15] performed the modal test of centrifugal compressor bladed wheels using a robotic arm to point the LDV automated on selected measurement locations. Multiple points can be measured by controlling the motion of the robotic arm, although the implementation method is complex.

In the modal tests, an excitation system is needed such as the vibration exciter or hammer. For the lightweight multiblade packet structures, the vibration exciter always introduced test error due to its added mass, and it is limited to the low usable frequency range: usually not more than 5 kHz. The broadband excitation frequency can hardly reach 10 kHz when metal head hammers are used. However, the energy attenuation of the excitation force of hammer is very fast at high frequencies so that the high natural frequencies of structures are difficult to get excited. Firrone and Berruti [16] designed an electromagnetic system for the noncontact excitation of bladed disks, and it allows obtaining a maximum of 5 N force amplitude for a mechanical frequency of about to 600 Hz. The blade packets are frequently subjected to failures caused by high-cycle fatigue when vibrating with high mode shapes, so that it is most important to be able to measure the vibration characteristics at high frequencies up to ten kHz.

In this paper, the developed test rig and procedure for measurements are presented in detail. The test rig is used to undertake the modal testing of a blade packet comprising 18 vane blades connected by shrouds. The measurements are performed within the high frequency range of 0–30 kHz, and the natural frequencies and mode shapes are obtained for first 97 modes. A laser vibrometer is used to measure the responses of the multiblade packets in a noncontact manner, while swept-sine signal generated by signal generator is applied to a loudspeaker to provide acoustic excitation [17] for the tested multiblades packet. In order to improve the signal-to-noise ratio and the frequency resolution, the modal tests are performed by the splitting of the whole frequency range of interest into several different frequency-bands. Moreover, a finite element model of the complex multiblade packet is created to compare with the natural frequencies and modal shapes obtained from the experiments.

2. Fundamentals of Modal Testing

2.1. System Configuration. The conventional excitation devices such as electromagnetic modal shakers and impact hammers have the difficulty to be used in the modal tests for frequencies over 10 kHz. To overcome the limitation, a noncontact acoustic excitation system that is composed of a high-frequency loudspeaker, signal generation, and power amplifier is applied to excite the multiblade packet.

A noncontact excitation and noncontact measurement scheme used for testing the modal properties of the blade packets is shown in Figure 1. The system consists of the computer, which has a built-in signal generator and data acquisition system, Scanning Laser Doppler Vibrometer (SLDV), power amplifier, and acoustic excitation. SLDV and the data acquisition system are used to collect vibration responses of the structure under acoustic excitation. The noncontact acoustic excitation is applied to avoid the adding constraint and mass of shaker transducer traditionally attached to the tested structure. The effect of distortion of the modal properties for the small and lightweight structures (which the bladed packets analyzed here are) is very significant and do not allow using the shaker excitation in our tests. The wide frequency range signal generated by the signal generator is amplified through a power amplifier and then submitted to the acoustic exciter. SLDV is used to acquire the vibration of the tested structure simultaneously with the acoustic exciter.

A multiblade packet, comprised of 18 vane blades connected by inner and outer shrouds is subjected to the modal testing (see Figure 2). The blade length is approximately 2.5 centimeters. The multiblade packet is suspended by two bungee cords at 1/3 and 2/3 length of the whole packet to simulate free boundary conditions. The boundary conditions can be considered as free boundary conditions since the highest frequency of rigid body modes of the packet in out-of-plane and in-plane mode measurements are much lower than 10% of the first elastic mode natural frequency of the blade packet, as recommended in [18]. In order to excite

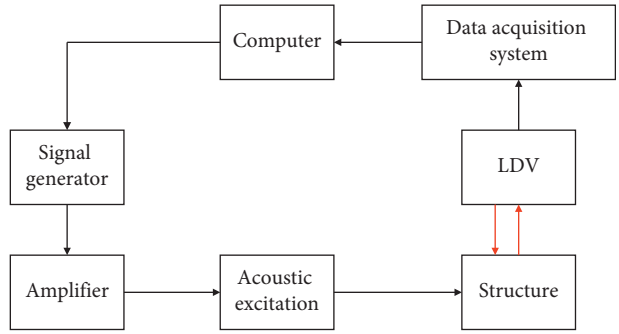

Figure 1: Configuration of the multiblade packet measurement system.

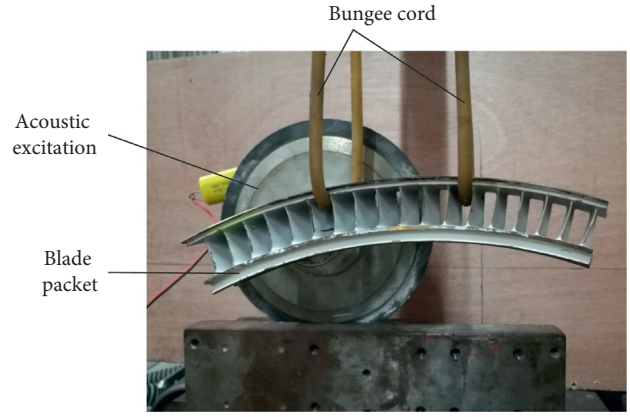

Figure 2: The experimental scheme.

the high frequency modes of the multiblade packet, an acoustic excitation with dynamic frequency response range of 2 kHz to 30 kHz is used in the tests. The excited modes and sound pressure applied to the blade packet is significantly affected by the location and distance between the acoustic exciter and the structure surface; therefore, it is necessary to adjust them between the emitting surface of the loudspeaker and the structure surface during the test. In our tests, the acoustic exciter is placed near 1/3 of the multiblade packet length at the distance between it and the blade packet about 1 centimeter (as shown in Figure 2).

2.2. Principle of LDV Measurements. The schematic configuration of a LDV is shown in Figure 3. The laser beam is split into two beams: (i) one beam is directed to structure surface and captured by the photodetector after being reflected from the surface; (ii) another beam is received directly by the photodetector from the beam splitter as a reference beam. The light reflected by the moving target is collected by the photodetector placed on the same part of the beam source with respect to the target structure. The mixing of the reflected light with the reference beam on the surface of the photodetector produces a heterodyne or beating signal of two frequencies in the output intensity of the photodetector electrical signal. It is possible to recover from this output signal the frequency shift f_D, between the measuring and reference beams pair caused by the Doppler effect.

The Doppler frequency shift resulting from the instantaneous motion of a measured point with velocity v along the direction comprising with of the laser beam angle θ is defined by the following relationship:

$$f_D = \frac{2v\cos(\theta)}{\lambda}, \tag{1}$$

where λ is the wavelength of laser beam (632.8 nm for a Helium-Neon laser source used in our experiments) and $v\cos(\theta)$ is the projection of the velocity of the vibrating surface at a measurement point in the laser beam direction.

2.3. Modal Analysis with Acoustic Excitation. In this paper, the LDV is used to obtain the vibration responses of the large number of the measurement points while the acoustic excitation provides a specific broadband excitation. Due to the nature of acoustics, the excitation is, generally, applied over some area rather than at a point, which contrasts the hammer or shaker excitation. The frequency response function (FRF) is obtained by dividing vibration response by input signal of force, and the FRF is a pseudofrequency function essentially. In [17], the characteristic of acoustic field is used to provide the reference force function, and results manifested the equivalence of acoustic and mechanical excitation for obtaining modal response. The smaller the aperture of the loudspeaker, the higher the frequency it can output; moreover, the characteristics of loudspeaker frequency are also dependent on the material

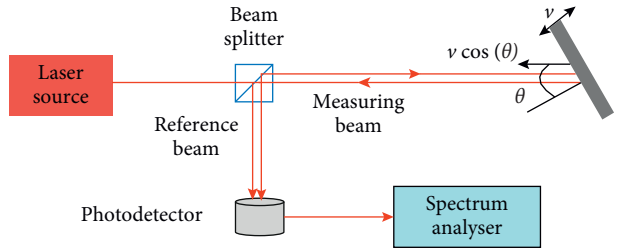

Figure 3: Basic LDV arrangement.

of the loudspeaker basin. In order to realize the high frequency excitation, a small-bore loudspeaker with a metal basin was chosen, and the small excited area on the structure can be regarded as close sufficiently to a point of excitation. From that has been discussed above, the pseudofrequency response functions are approximately equal to the FRFs.

The motion equation of a structure is described as

$$M\ddot{x}(t) + C\dot{x}(t) + Kx(t) = F(t), \tag{2}$$

where M, C, and K are the mass matrix, damping matrix, and stiffness matrix, respectively, and $F(t)$ is the excitation force vector.

The vibration response solution can be directly written as

$$X = (K - \omega M + i\omega C)^{-1} F = H(\omega) F, \tag{3}$$

where $H(\omega)$ is defined as the receptance frequency response function (FRF) matrix of the system. A more explicit form of this solution may be derived as

$$X = \sum_{r=1}^{N} \frac{\phi_r^T F}{\omega_r^2 - \omega^2 + i2\zeta_r\omega_r\omega}\phi_r, \tag{4}$$

where ω_r, ϕ_r, and ζ_r are natural frequency, mode shape, and the critical damping ratio for the rth mode. The vectors of response X are regarded as the operating deflection shapes (ODS). It can be seen that the ODS is the function of the excitation force and modal properties such as natural frequencies, damping, and mode shapes. The excitation force that is often used in modal test of aerospace structures is the swept-sine excitation force treated as a broad-band excitation [19]. In this paper, the excitation force $F(t)$ generated by the signal generator is a swept-sine function [20, 21], which leads to a time-dependent excitation force of

$$F(t) = A\sin\left[2\pi\left(f_1 t + \frac{1}{2}at^2\right)\right], \tag{5}$$

where A is the amplitude of force; a is the frequency sweep rate; and f_1 is the starting excitation frequency. The frequency sweep rate can be determined from the time interval T chosen for the frequency sweeping test and the desired excitation frequency at the beginning, f_1, and end, f_2, of this interval:

$$a = \frac{(f_2 - f_1)}{T}. \tag{6}$$

3. Measurement of the Multiblade Packet

3.1. Experimental Setup. To obtain the detailed information about blade mode shapes in the packet for high order modes, which can experience high level of localization of the amplitudes, a significant number of measurement points are required for each blade. In our measurements, 5°×°5 measurement points were arranged at each blade. In addition, 19 measurement points are selected uniformly distributed along the lengths of each of the two shrouds. The total number of measurement points for the blade packet is 488, as shown in Figure 4. The scanning measurements are used when the LDV automatically scans all these points sequentially. In our tests, the LDV is placed sufficiently far from the blade packet, and the laser beam is oriented to be approximately normal to the concave surfaces of the blades in order to have all blades visible by the laser beam and allow the blade measurements without overshadowing by neighboring blades. The multiblade packet's surface is coated with a spray provided by the LDV manufacturer, in order to increase the diffusivity of the beam reflection and the intensity of the reflected light [22].

The laser beam signal obtained from LDV and transformed by the photodetector into an electrical signal is a continuous variable voltage signal that requires to be digitized. Generally, the sampling must be performed at a frequency rate of at least twice the highest frequency component of interest according to Nyquist's sampling rule. To avoid "aliasing", antialiasing filters are used. Because the filters used are inevitably less than perfect and have a finite cutoff rate, it means that the higher frequency range approaching the Nyquist values still has the possibility to be aliased. For the complete antialiasing, the sampling frequency is selected 2.56 times of the highest frequency component of interest (30 kHz). The number of spectral lines usually determined the frequency resolution of analysis. The higher the frequency resolution is, the more the spectral lines are required. The maximum number of spectral lines in the PSV data acquisition of Polytec-PSV-400 is currently 6400, which is used in our tests to obtain the highest possible frequency resolution. For the frequency range of the measured signal obtained under the acoustic excitation in the frequency range from 5 Hz to 30 kHz the frequency resolution is

$$\Delta F = \frac{F_{\max}}{M}, \tag{7}$$

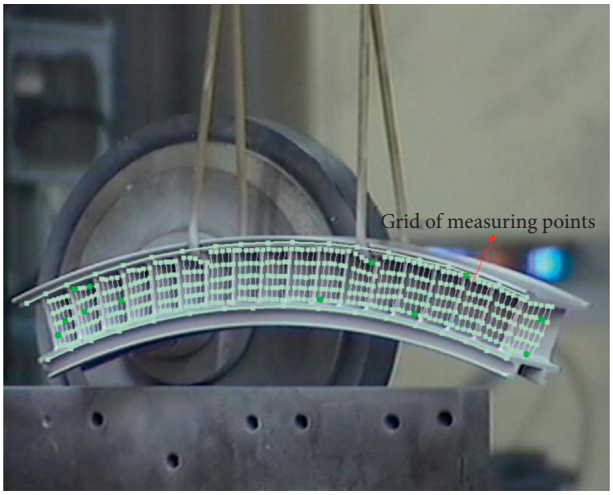

Figure 4: Measurement points used in the experiment.

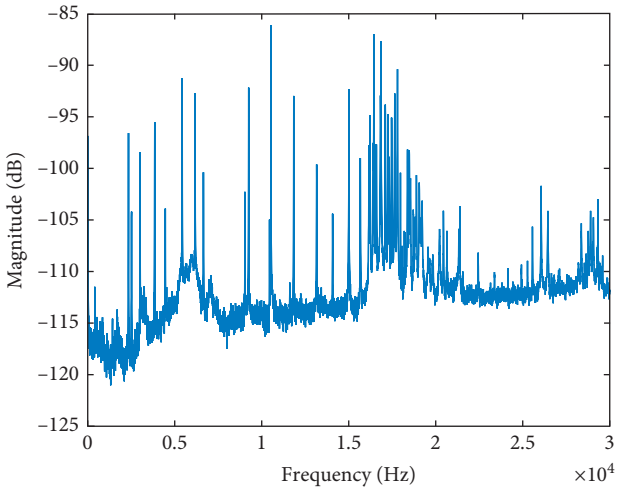

Figure 5: The averaged pseudofrequency response function.

where F_{max} is the maximum analyzed frequency and M is the number of spectral lines. The frequency resolution $\Delta F = 4.6875$ Hz.

During a frequency sweep excitation, all resonances of the structure in the analysed frequency range are passed within the test time T. Thus, the test time of frequency sweeping can be defined as

$$T = \frac{2.56^{*}M}{F_{\text{sample}}} = \frac{2.56^{*}M}{2.56^{*}F_{\text{max}}} = \frac{1}{\Delta F}. \quad (8)$$

For each measurement point, the tests are repeated three times to be averaged after processing the results. As the laser scans step by step over the grid of 488 points (see Figure 4), the total test time can be derived as follows without considering the time interval of laser point from one measurement position to the next:

$$T_{\text{total}} = T \times n.\ \text{of averagings} \times N = \frac{1}{4.6875} \times 3 \times 488 = 312.32\,(s), \quad (9)$$

Table 1: Frequency bandwidth and frequency resolution.

No.	$(f_1 \sim f_2)$ (Hz)	ΔF (Hz)	T (s)	a (Hz/s)
1	0–5000	0.7813	1.28	3906
2	5000–10000	1.5625	0.64	7813
3	10000–15000	2.3438	0.43	11628
4	15000–20000	3.1250	0.32	15625
5	20000–25000	3.9063	0.256	19531
6	25000–30000	4.6875	0.213	23474

where N is the number of measurement points and n is the number of measurements to be averaged. Generally, it is necessary to perform an averaging process to obtain a reliable result. The two major considerations which determine the number of the required averages are the statistical reliability and the removal of spurious random noise from the signals. To this end, three individual time records are performed for each measurement point.

The high-frequency loudspeaker selected in this paper for noncontact excitation has good dynamic performance in

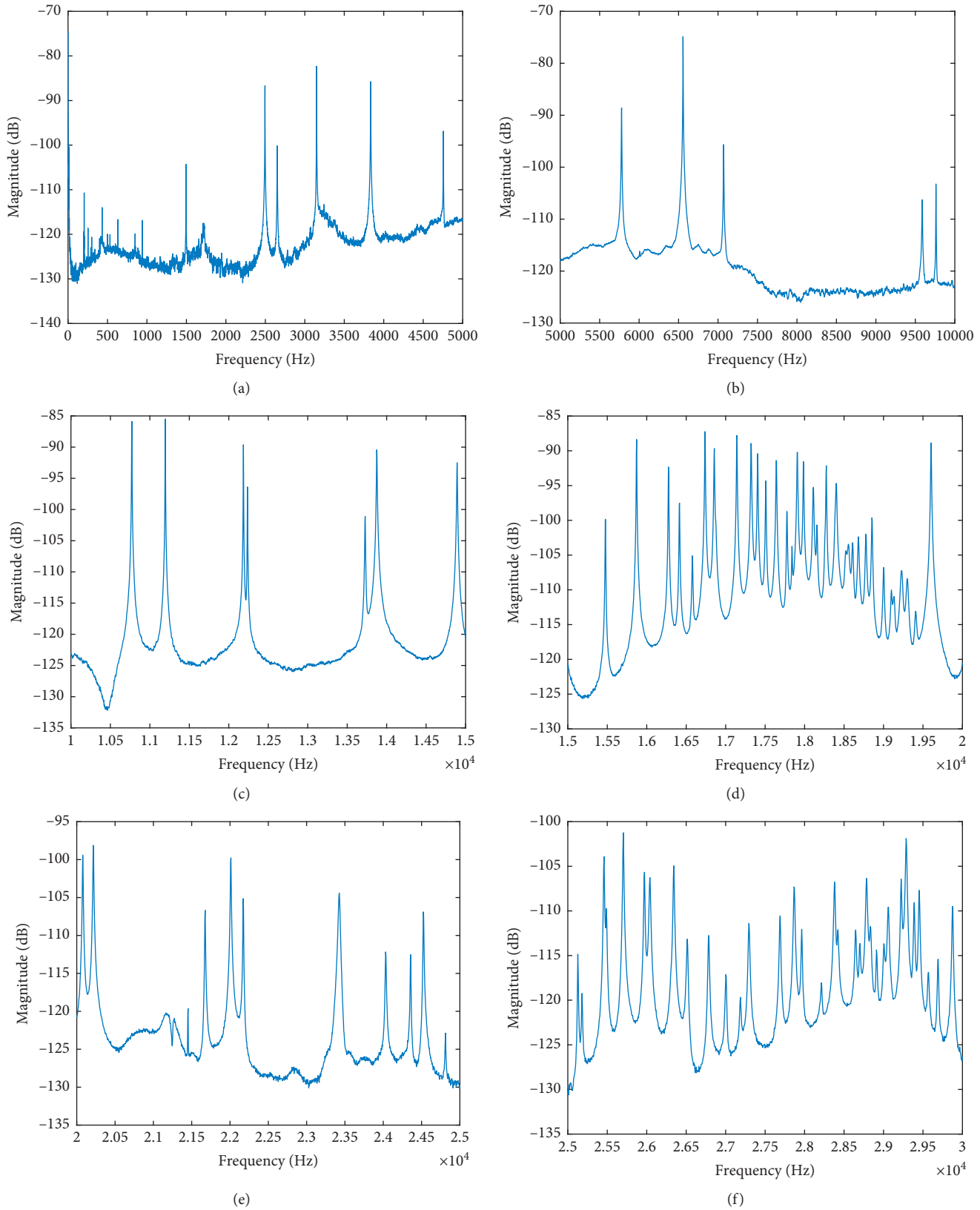

Figure 6: Measured FRFs (averaged over 3 tests). (a) 0–5 kHz. (b) 5–10 kHz. (c) 10–15 kHz. (d) 15–20 kHz. (e) 20–25 kHz. (f) 25–30 kHz.

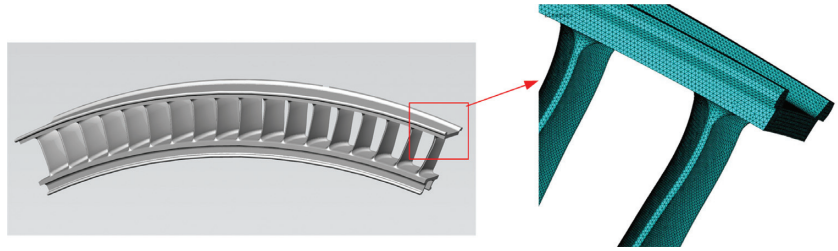

Figure 7: FEM model of the multiblade packet.

the frequency range from 2 kHz to 30 kHz. For each measurement point, the tests were repeated three times. The pseudofrequency functions were then obtained and averaged each time in order to minimize the effects of noise on the results of measurements. Figure 5 shows the average pseudo-FRF of all measurement points.

Because the frequency resolution of abovementioned measurement is relatively low ($\Delta F = 4.6875$ Hz), it is difficult to identify the cluster of natural frequencies which are typical for blade packets. On the other hand, the noise level within the frequency bandwidth is high as shown in Figure 5 because the structure is excited by the swept-sine signal in a rather short time and the fast sweep rate of the excitation signal does not allow strong excitation for the structure. The spectral energy of the swept-sine excitation within its analyzed frequency band can be controlled by two parameters: excitation amplitude (A) and the frequency sweep rate (a). Therefore, the excitation energy can be controlled by arbitrarily setting the amplitude A according to equation (5) or determined by the frequency sweep rate a. The analytic expression for the normalized Fourier spectrum (NFS) of the swept-sine signal can be expressed as [19]

$$|\mathrm{NFS}| = A\,(2\pi a)^{-1/2}. \tag{10}$$

It can be summarized that the sweep rate is a parameter that is able to determine the excitation level as well as the force amplitude. In order to ensure enough energy to excite most of the modes of the multiblade packet, the small frequency band $(f_2 - f_1)$ and the long test time are desired to reduce the sweep rate a. To overcome these problems of both the low frequency resolution and the high noise level, one easy approach is to divide the measurement task over the frequency range of 30 kHz into several tests performed for the split frequency bandwidths. Besides, as the whole testing takes a relatively long time, the repeatability of certain FRFs are measured from time to time, just to check that if the structure or the measurement system have experienced any significant changes. In this way, the quality of measured data is ensured.

3.2. Modal Testing with the Frequency Range Splits. For the multiblade packet mentioned above, the analyzed frequency range of 0–30 kHz was split in 6 frequency bandwidths with the frequency interval length of 5 kHz for each of them in order to obtain a higher frequency resolution and to have the enough excitation energy. This approach is referred as the subband modal test in this paper. With 6400 spectral lines in each subband, the frequency resolution and the test time for each point can be calculated by substituting the maximum frequency of every subband into equation (6). The values of frequency resolution, the time of test interval for each measurement point, and the frequency change rate are given in Table 1. Comparing with the direct test of the whole frequency band discussed in Section 3.1, the higher frequency resolution (except for the sixth sub-band) and slower sweep rate are obtained.

The averaged pseudofrequency response functions measured in the six frequency bands are plotted in Figure 6. Except for the first frequency band in the range of 0–5 kHz, FRFs of all frequency bandwidths for modal analysis have high signal-to-noise ratios. It is obvious that more modes in the FRFs are excited and most of them are rather clear. It also can be found in Figure 6(a) that more noise existed below 2 kHz. That is mainly caused by the limitation of the high frequency loudspeaker's performance (it has a good performance in the frequency range from 2 to 30 kHz). The resonance frequencies in frequency range 15–30 kHz shown in Figures 6(d)–6(f) are denser than the modes in the range of 0–15 kHz band shown in Figures 6(a)–6(c)). It is because more local modes caused by blades vibration were excited, which usually complicate the vibrational characteristics of multiblade packet in high-frequency modes. Although the frequency resolution of the sixth test in frequency range from 25 to 30 kHz is not been improved, the excitation energy has significantly increased.

4. Discussion of Results

4.1. Finite Element Simulation. To verify the experimental results, the modal analysis of the multiblade packet using finite element analysis (FEA) is made. The finite element model of the multiblade packet was built in ANSYS using 19.54 million nodes and 12.97 million finite elements as shown in Figure 7. The SOLID187 element used in the modelling is a quadratic approximation three-dimensional solid element with 10 nodes. Such a large finite element model is created in order to ensure the high-fidelity modeling for the high natural modes and to avoid any questions related to the possible mesh convergence errors. The geometry shape of the blade packet was taken from CAD-generated files provided by the manufacturer of the blade packet. The CAD model describes the geometry that is designed and intended to be manufactured, but the actual packet geometry was not measured and the discrepancies from the actual test piece geometry within manufacture tolerances are possible.

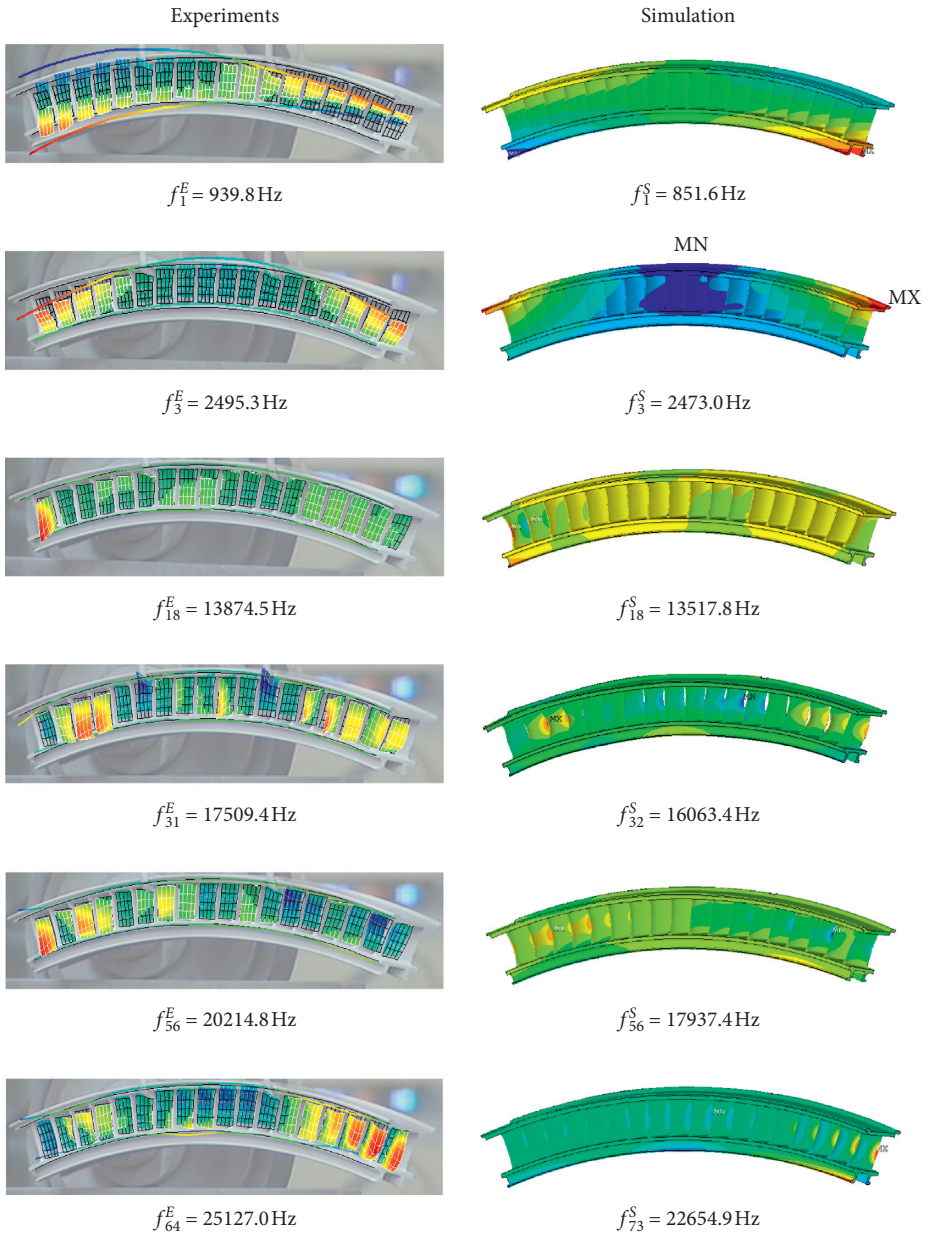

Figure 8: Comparison of experimental and simulated mode shapes and natural frequencies.

Young's modulus of the material is 199.9 GPa, and the material density is 8240 Kg/m^3. The modal analysis of the structure under free boundary conditions is carried out by the Lanczos method. First 97 modal frequencies and mode shapes are calculated for the comparison with measured values. Due to the complexity of the multiblade packet, results from the numerical model may not always exactly describe the actual structure. Nevertheless, the numerical results can be used to verify the correctness of experimental data and help to check whether the missing modes existed in the experimental test.

4.2. Comparison between Experiments and Simulation. Because of the complexity of multiblade packet vibration, there are nearly a hundred of modes within 0–30 kHz frequency range analyzed here. For the sake of brevity, only some representative mode shapes are shown below. The comparison of mode shapes obtained from numerical simulation and measurements are shown in Figure 8, where the experimental mode shapes are presented in the left column and the simulated mode shapes using FEA are given in the right column. The natural frequencies from the experiment and the simulation: f_r^E and f_r^S (r is the number of mode), respectively, are shown here too. The experimental measurement results demonstrate a good correspondence with the simulated results. The numerical results from simulation show that the first 16 modes of the multiblade packet are dominated by bending and torsional modes of the whole packet. Comparing the 1st mode and the 3rd mode as examples, they are torsional and bending vibrations of the whole structure, respectively. After the 16th mode, the mode

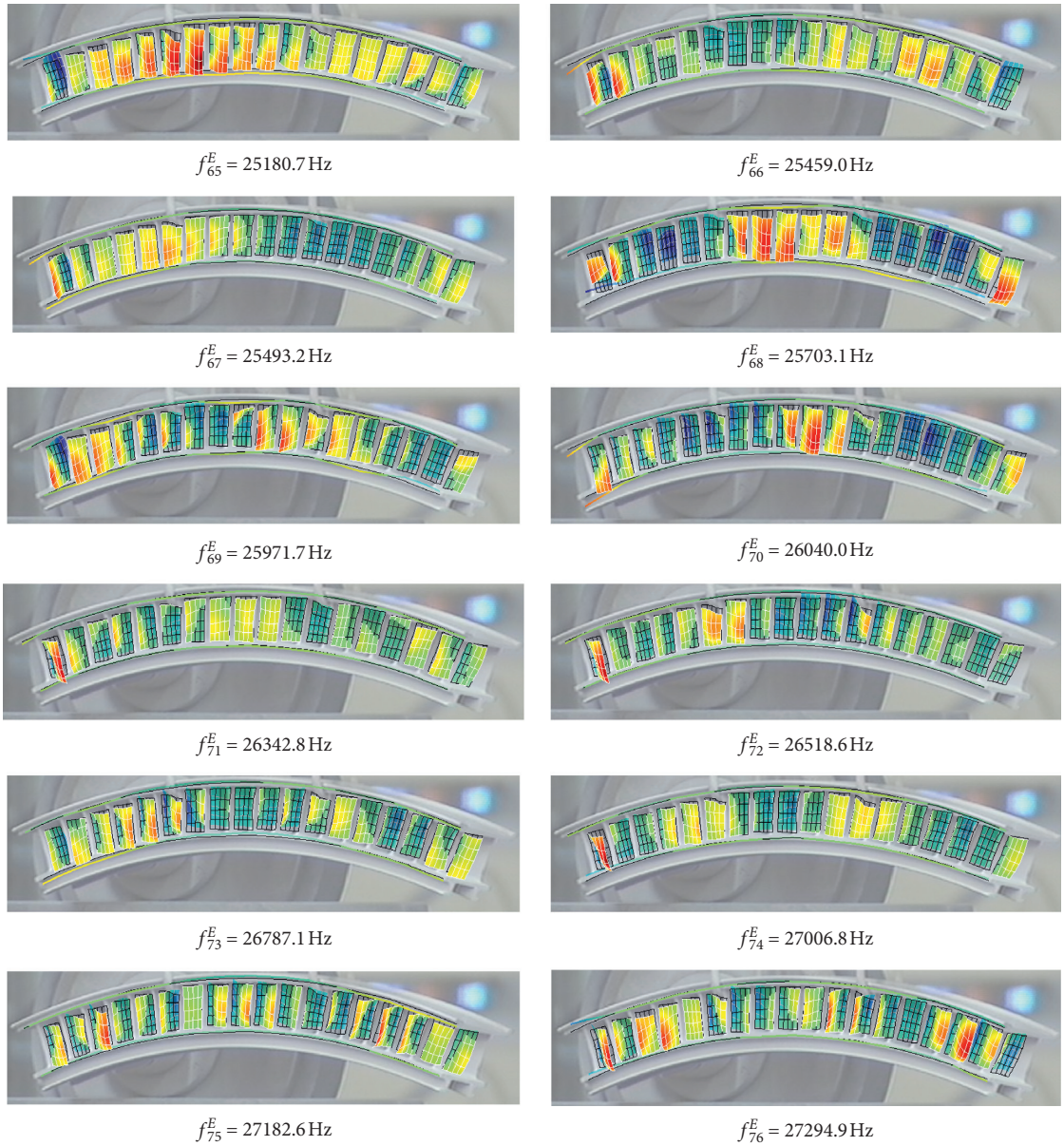

Figure 9: Natural frequencies and mode shapes for modes from 65th to 76th.

shapes are mainly dominated by the localized vibrations of blades and coupled shroud-blade vibrations. The localized vibration caused by one blade is also a typical form of multiblade packet's vibration, like as the 18th mode shape shown in Figure 8. The vibration is concentrated on the first blade at the left end, which will be disadvantageous to the safe operating of the rotating machine. The more common type of vibration modes is the coupling vibration by several blades as the 32, 56, and 73 mode shapes demonstrated in Figure 8.

Many experimentally measured mode shapes and natural frequencies are in good correspondence with the simulation results especially for the low frequency modes. For modes higher than 16, it is more difficult to match the experimental mode shapes with the simulation results. There are two major reasons for this: (i) the blade packet manufacturing is not perfect, and its actual geometry may differ from the geometry designed and reflected in our finite element model created from the CAD files; (ii) some of the blade packet highly localized modes did not produce high-resonance peaks in the experiments. and one-by-one natural frequency correspondence between numerical and measured natural frequencies was hindered.

The natural frequency and mode shape measurements have been performed for all first 97 modes. Due to restrictions on the size of the paper, they cannot be presented all here, and, as an example, a set of 24 measured mode shapes of higher modes, from 65th to 88th, are shown in Figures 9 and 10. One can see that most of these modes have highly localized mode shapes, although some of the modes are due to vibration of the blade packet as a whole structure (e.g., see 65th mode shape).

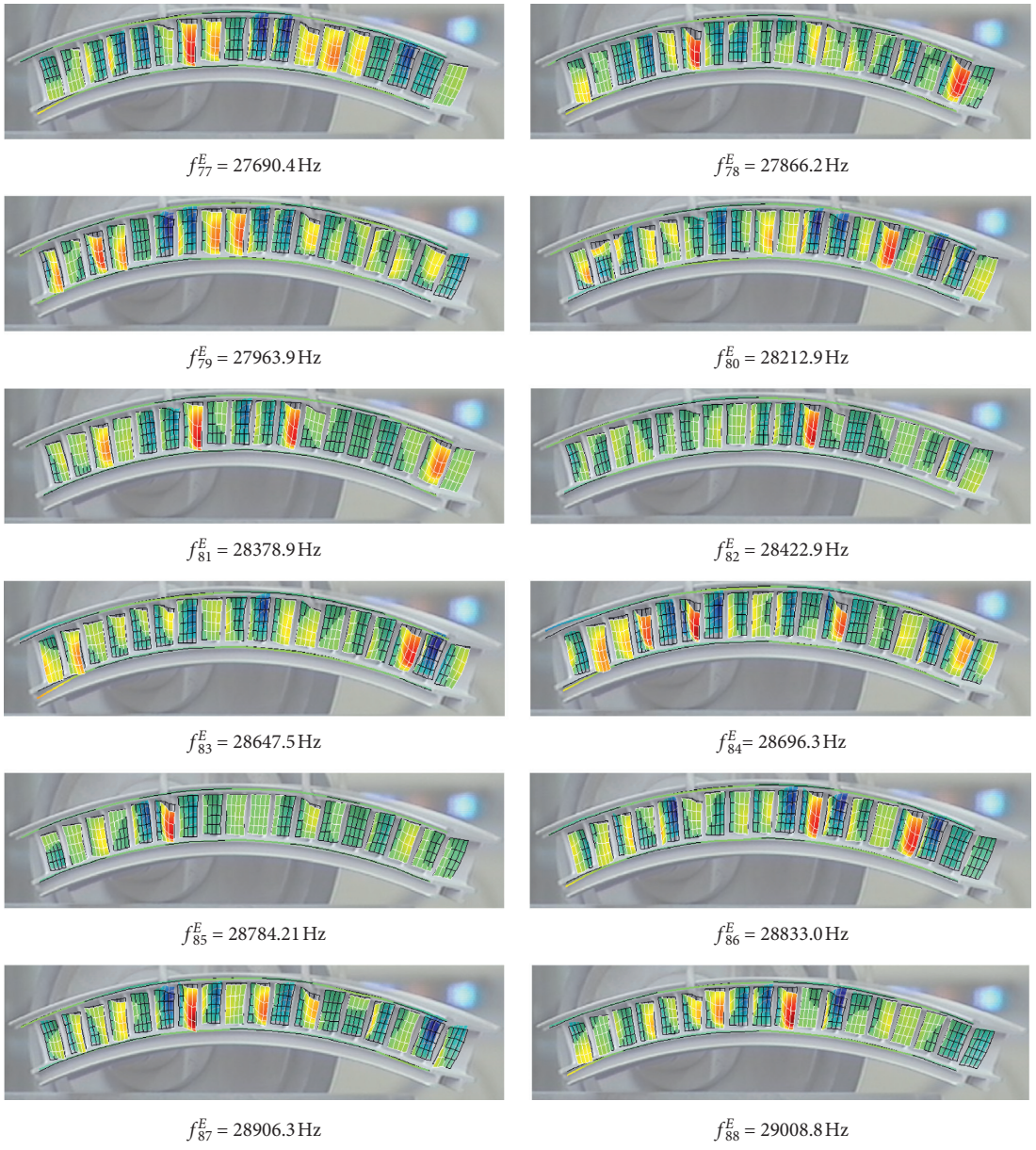

Figure 10: Natural frequencies and mode shapes for modes from 77th to 88th.

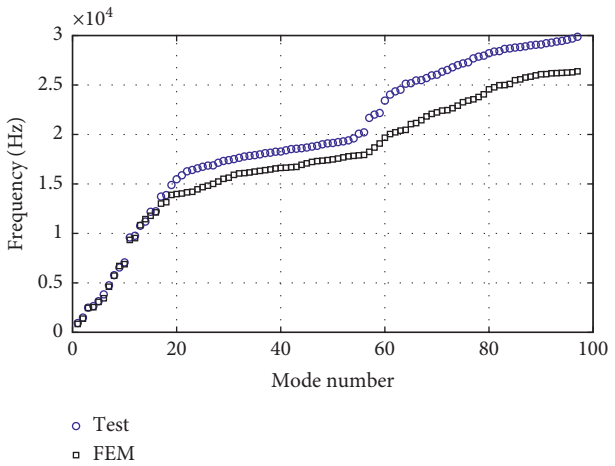

Figure 11: Modal frequencies of measurements and simulation.

Natural frequencies of the multiblade packet are shown in Figure 11 for all found by modal testing and by numerical modelling modes. It is evident that the first 16 modal frequencies from experimental tests are in agreement with the results from FEA and the frequency gap between the two is getting wider with the increase of frequency after the 16th mode. Results illustrate that the finite element analysis, for multiblade packets, can effectively predict low frequency modes, but the prediction of the high-frequency modes has some difficulty. The large number of the blades interacting through the shrouds makes the vibrational characteristics of multiblade packets too complex to predict for high modes, especially with accounting for the small scatters of the blade geometry from the drawings. Taking into account, that the vibration failure, like blade crack and even break off, in many cases, occurs at higher modes, the effective measurement for the multiblade packet structure is of great significance. On the other hand, the capability of the proposed measurement method is validated here by comparing the results between experiments and simulation.

5. Conclusions

In this paper, the test rig and procedure for measurements of dynamic characteristics of lightweight multiblade packets have been developed. The measurements are based on a noncontact excitation and noncontact measurement method, which allows the determination of the modal characteristics of the packets with high accuracy in wide frequency ranges. The responses of the multiblade packets are measured using a scanning laser Doppler vibrometry, while vibrations are excited by the acoustic excitation technique. In order to obtain the high frequency resolution, the subband test method is proposed when the frequency range used for the measurements is split into several frequency intervals according to the number of spectral lines available in the used data acquisition system.

As an example, the modal characteristics of a blade packet comprising 18 vane blades connected by shrouds measured within the high frequency range of 0–30 kHz and the natural frequencies and mode shapes are obtained for the first 97 modes. To capture the complex high frequency blade mode shapes, each blade in the packet is scanned over 25 reference points uniformly distributed over the blade concave surface. Results show that the low frequency modes of the multiblade packet are mostly dominated by the whole structure's vibration and the high frequency modes are dominated by local vibrations or coupling vibrations of multiblades.

The finite model of the packet is created, and the numerical modal analysis is performed to compare calculated natural frequencies and mode shapes with the experimental measurements. The comparison shows the satisfactory correspondence of numerical and experimental results in a significantly wide frequency range, although for very high frequencies noticeable discrepancies occur.

The obtained results demonstrate that the developed technique allows effective modal test measurements for the multiblade packets and other structures for high order modes.

Data Availability

As the data from the measurement of the real component of one type of aeroengine are still on service, they are currently treated confidential.

Conflicts of Interest

The authors declare no conflicts of interest.

Acknowledgments

The authors gratefully appreciate the financial support for this work provided by the National Natural Science Foundation of China and National Safety Academic Foundation of China (no. U1730129) and the Cultivation Foundation of National Defense Large Projects of China (no. NP2018450). The supports from Jiangsu Province Key Laboratory of Aerospace Power System, the Key Laboratory of Aero-Engine Thermal Environment and Structure, and Ministry of Industry and Information Technology are also gratefully acknowledged.

References

[1] J. S. Rao, "Turbomachine blade vibration," *Shock & Vibration Digest*, vol. 15, no. 5, pp. 3–9, 1991.

[2] A. Oberholster and S. Heyns, "A study of radial-flow turbomachinery blade vibration measurements using Eulerian Laser Doppler Vibrometry," in *Proceedings of 11th International Conference on Vibration Measurements by Laser and Noncontact Techniques-AIVELA 2014: Advances and Applications*, American Institute of Physics, Ancona, Italy, June 2014.

[3] P. Beauseroy and R. Lengellé, "Nonintrusive turbomachine blade vibration measurement system," *Mechanical Systems and Signal Processing*, vol. 21, no. 4, pp. 1717–1738, 2007.

[4] D. J. Ewins and M. Imregun, "Vibration modes of packeted bladed disks," *Journal of Vibration and Acoustics*, vol. 106, no. 2, pp. 175–180, 1984.

[5] J. Thomas and H. T. Belek, "Free vibration of blade packets," *Journal of Mechanical Engineering Science*, vol. 19, no. 1, pp. 13–21, 1977.

[6] W. Huang, "Free and forced vibration of closely coupled turbomachinery blades," *AIAA Journal*, vol. 19, no. 7, pp. 918–924, 2015.

[7] H. S. Lim, J. Chung, and H. H. Yoo, "Modal analysis of a rotating multi-packet blade system," *Journal of Sound and Vibration*, vol. 325, no. 3, pp. 513–531, 2009.

[8] K. Uchino, T. Kamiyama, T. Inamura et al., *Three-Dimensional Photoelastic Analysis of Aeroengine Rotary Parts. Photoelasticity*, pp. 209–214, Springer Japan, Tokyo, Japan, 1986.

[9] D. S. Delhelay, *Nonlinear Finite Element Analysis of the Coupled Thermomechanical Behaviour of Turbine Disc Assemblies*, National Library of Canada°=°Bibliothèque nationale du Canada, Ottawa, Canada, 2001.

[10] Y. Ma, W. Chen, Y. Wang et al., "Finite element model updating of a blade swing mechanism based on response surface method," *Journal of Vibration and Shock*, vol. 35, no. 22, pp. 232–236, 2016.

[11] A. Chatterjee and M. S. Kotambkar, "Modal characteristics of turbine blade packets under lacing wire damage induced

mistuning," *Journal of Sound and Vibration*, vol. 343, pp. 49–70, 2015.

[12] Y. Duan, C. Zang, and E. Petrov, "Forced response analysis of high-mode vibrations for mistuned bladed discs with effective reduced-order models," *Journal of Engineering for Gas Turbines and Power*, vol. 138, pp. 1–11, 2016.

[13] W. Tang, B. I. Epureanu, and S. Filippi, "Models for blisks with large blends and small mistuning," *Mechanical Systems and Signal Processing*, vol. 87, pp. 161–179, 2017.

[14] J. C. Slater, G. R. Minkiewicz, and A. J. Blair, "Forced response of bladed disk assemblies--a survey," *The Shock and Vibration Digest*, vol. 31, no. 1, pp. 17–24, 1999.

[15] L. Bertini, P. Neri, C. Santus, and A. Guglielmo, "Automated experimental modal analysis of bladed wheels with an anthropomorphic robotic station," *Experimental Mechanics*, vol. 57, 2017.

[16] C. M. Firrone and T. Berruti, "An electromagnetic system for the non-contact excitation of bladed disks," *Experimental Mechanics*, vol. 52, no. 5, pp. 447–459, 2012.

[17] B. G. Musson and J. R. Stevens, "Comparison of acoustic and mechanical excitation for modal response measurements," in *Proceedings of the 3rd International Modal Analysis Conference*, vol. 1, pp. 124–130, Union College, Orlando, FL, USA, January 1985.

[18] D. J. Ewins, *Modal Testing: Theory and Practice*, Research Studies Press, Boston, MA, USA, 1984.

[19] G. Gloth and M. Sinapius, "Analysis of swept-sine runs during modal survey and qualification tests," *Journal of the Japan Welding Society*, vol. 581, no. 3, p. 60, 2005.

[20] A. Farina, *Simultaneous Measurement of Impulse Response and Distortion with a Swept-Sine Sechnique*, Vol. 108, Audio Engineering Society Convention, New York, NY, USA, 2000.

[21] M. Rowe, "Generate a swept sine test signal," *Test & Measurement World*, vol. 20, no. 12, p. 21, 2000.

[22] M. Martarelli, *Exploiting the Laser Scanning Facility for Vibration Measurements*, University of London, London, UK, 2001.